Crystal chemistry of silica-rich Barium silicates

III: Refinement of the crystal structures of the layer silicates $Ba_2[Si_4O_{10}]$ (I), (Sanbornite), and $Ba_2[Si_4O_{10}]$ (h)

K.-F. Hesse and F. Liebau

Mineralogisches Institut der Universität,
Olshausenstr. 40/60, D-2300 Kiel, Federal Republic of Germany

Abstract. The crystal structures of the two title compounds have been refined with three-dimensional $MoK\alpha$ X-ray intensities. Results for both are given in the order a, b, c, β, Z, space group, number of independent reflections, R(unweighted), R(weighted):

$Ba_2[Si_4O_{10}]$ (l): 7.688(1) Å, 4.629(1) Å, 13.523(1) Å,
90°, 2, $Pmcn$, 611, 0.041, 0.045.

$Ba_2[Si_4O_{10}]$ (h): 23.195(2) Å, 4.658(1) Å, 13.613(1) Å,
97.57(1)°, 6, $C2/c$, 1579, 0.033, 0.034.

Both polymorphs contain chains with two $[SiO_4]$ tetrahedra in the repeat unit of approximately 4.6 Å (*zweier* single chains). These chains are linked via every second tetrahedron to *zweier* single layers parallel (001). The higher degree of corrugation of the layers in the low-temperature phase compared to those of the high-temperature phase is explained by the smaller effective radius of the barium ions at lower temperature. Barium ion coordination number is 9 in the low-temperature and both 9 and 8 + 2 in the high-temperature form respectively. The barium oxygen polyhedra share edges to form layers parallel (001).

Introduction

In the course of a more extensive study of silica-rich barium silicates (Hesse and Liebau, 1980; Czank and Buseck, 1980; Liebau, 1980) the crystal structures of both the low-temperature phase $Ba_2[Si_4O_{10}]$ (l), known as the mineral sanbornite, and the synthetic high-temperature phase $Ba_2[Si_4O_{10}]$ (h) were refined. In this paper the refinements and their results are briefly described. A comparison of these structures with those of the chain silicates $Ba_2[Si_2O_6]$ (h) (Grosse and Tillmanns, 1974), $Ba_4[Si_6O_{16}]$, $Ba_5[Si_8O_{21}]$ and

$Ba_6[Si_{10}O_{26}]$ (Hesse and Liebau, 1980) and a more detailed discussion in connection with the condensation of single chains to multiple chains and layers will be given in a separate paper (Liebau, 1980).

Experimental

Single crystals of sanbornite from Fresno County, California, USA, were kindly supplied by Professor A. Pabst, Berkeley; those of $Ba_2[Si_4O_{10}]$ (h) were grown by solid state reaction of a stoichiometric mixture of $BaCO_3$ and SiO_2 at 1400°C for two days. Lattice constants were refined (Table 1) and intensities measured on an automatic Philips PW 1100 four-circle diffracto-meter (for experimental details see Hesse and Liebau, 1980). Least squares refinements were started with approximate atomic coordinates determined by Douglass (1958) for sanbornite and by Katscher, Bissert and Liebau (1973) for $Ba_2[Si_4O_{10}]$ (h). The program system SHELX-76 was used for the refinement. Scattering factors for ionized atoms were taken from International Tables for X-ray Crystallography Vol. IV. The final values of $R = \Sigma ||F_o| - |F_c||/\Sigma |F_o|$ and $R_w = [\Sigma w (|F_o| - |F_c|)^2/\Sigma wF_o^2]^{1/2}$, ($w = 1/\sigma^2$), for anisotropic refinement are given in Table 1 together with further experimental data. Final atomic parameters are listed in Table 2, bond

Table 1. Cell dimensions, space groups and details for the structure determination of barium phyllosilicates

	$Ba_2[Si_4O_{10}]$ (l)	$Ba_2[Si_4O_{10}]$ (h)
a [Å]	7.688(1)	23.195(2)
b [Å]	4.629(1)	4.658(1)
c [Å]	13.523(1)	13.613(1)
β [°]	—	97.57(1)
Z	2	6
Space group	$Pmcn$	$C2/c$
ϱ_c [g/cm³]	3.77	3.74
Size [nm]	$0.043 \times 0.100 \times 0.175$	$0.100 \times 0.075 \times 0.130$
μ [cm^{-1}]	88.8	88.8
Number of non-equivalent reflections with $|F_o| > 3\sigma$	611	1579
R	0.041	0.033
R_w	0.045	0.034
Parameters refined	39	108

Table 2. Final fractional atomic coordinates and thermal parameters for sanbornite, $Ba_2[Si_4O_{10}]$ (l), and $Ba_2[Si_4O_{10}]$(h). Estimated standard deviations in parentheses. U_{ij} are expressed for $T = \exp[-2\pi^2 (U_{11} h^2 a^{*2} + \ldots + 2 U_{12} hka^* b^* + \ldots)]$ in units [Å²]

Atom	x	y	z	U_{11}	U_{22}	U_{33}	U_{23}	U_{13}	U_{12}
$Ba_2[Si_4O_{10}]$ (l)									
Ba	$\frac{1}{4}$	0.7846(2)	0.5444(1)	0.0058(3)	0.0089(4)	0.0108(4)	0.0008(4)	—	—
Si	0.4518(4)	0.8626(6)	0.8166(2)	0.0035(11)	0.0044(13)	0.0100(13)	−0.0003(10)	0.0002(10)	−0.0001(10)
O(1)	$\frac{1}{4}$	0.9520(23)	0.8382(8)	0.0012(13)	0.0144(36)	0.0201(57)	0.0050(46)	—	—
O(2)	0.5368(8)	0.7404(15)	0.9127(4)	0.0097(29)	0.0079(33)	0.0138(29)	−0.0022(31)	0.0001(26)	0.0018(32)
O(3)	0.4485(9)	0.6559(14)	0.7189(5)	0.0093(31)	0.0078(36)	0.0112(33)	0.0022(26)	−0.0010(29)	0.0032(28)
$Ba_2[Si_4O_{10}]$ (h)									
Ba(1)	0	0	$\frac{1}{2}$	0.0058(3)	0.0104(4)	0.0108(3)	—	0.0005(2)	—
Ba(2)	0.1638(1)	0.5474(1)	0.9357(1)	0.0080(2)	0.0113(2)	0.0101(2)	0.0006(2)	0.0023(2)	0.0000(2)
Si(1)	0.0667(1)	0.1052(5)	0.7710(2)	0.0036(9)	0.0074(10)	0.0094(10)	−0.0003(8)	0.0010(8)	0.0000(8)
Si(2)	0.1022(1)	0.5880(5)	0.6506(2)	0.0043(9)	0.0069(10)	0.0085(9)	0.0000(8)	0.0002(8)	−0.0007(8)
Si(3)	0.2372(1)	0.6227(5)	0.6798(2)	0.0047(10)	0.0075(10)	0.0081(10)	−0.0005(8)	0.0011(8)	−0.0003(8)
O(1)	0	0.2237(18)	$\frac{3}{4}$	0.0025(37)	0.0103(40)	0.0405(52)	—	0.0010(35)	—
O(2)	0.0865(2)	0.9954(13)	0.8791(4)	0.0134(26)	0.0169(31)	0.0106(25)	0.0044(26)	0.0019(21)	0.0032(25)
O(3)	0.1071(2)	0.3828(12)	0.7486(4)	0.0034(25)	0.0085(27)	0.0159(28)	0.0032(23)	−0.0002(21)	−0.0020(21)
O(4)	0.0708(2)	0.8819(12)	0.6804(4)	0.0188(32)	0.0097(28)	0.0159(30)	−0.0032(25)	0.0007(25)	0.0023(24)
O(5)	0.0700(2)	0.4684(12)	0.5506(4)	0.0088(24)	0.0105(27)	0.0109(24)	−0.0026(24)	−0.0019(20)	−0.0027(23)
O(6)	0.1690(2)	0.6748(14)	0.6357(5)	0.0034(26)	0.0314(36)	0.0209(32)	0.0109(30)	−0.0022(23)	−0.0044(26)
O(7)	0.2705(2)	0.5100(13)	0.5947(4)	0.0117(26)	0.0120(28)	0.0108(25)	0.0025(25)	0.0040(21)	0.0050(23)
O(8)	0.2380(2)	0.4366(13)	0.7817(4)	0.0196(29)	0.0128(29)	0.0152(27)	−0.0043(26)	0.0063(23)	0.0015(26)

Table 3. Interatomic distances (in Å) and bond angles (in °) in $Ba_2[Si_4O_{10}]$ (l). (Standard deviations in parentheses.) O*: bridging oxygen atoms

[SiO_4] tetrahedra

Si—O distances		O—O distances		O—Si—O angles	
Si(1)—O(2)	1.561(7)	O(3)*—O(3)*	2.587(9)		104.9(0.4)
—O(3)*	1.630(7)	O(1)*—O(3)*	2.609(11)		106.2(0.5)
—O(3)*	1.631(7)	O(1)*—O(2)	2.614(8)		109.8(0.5)
—O(1)*	1.632(4)	O(1)*—O(3)*	2.620(9)		106.8(0.5)
mean	1.614	O(2) —O(3)*	2.623(9)		110.5(0.4)
		O(2) —O(3)*	2.735(9)		117.9(0.4)
		mean	2.631	mean	109.4

Si—O—Si angles

Si(1)—O(3)*—Si(1)	136.0(1.2) (2×)
Si(1)—O(1)*—Si(1)	143.8(0.9)
mean	138.6

[BaO]_n polyhedra

Ba(1)—O(2)	2.734(7)
—O(2)	2.734(7)
—O(2)	2.836(6)
—O(2)	2.836(6)
—O(3)*	2.873(7)
—O(3)*	2.873(7)
—O(1)*	2.995(11)
—O(2)	3.061(7)
.—O(2)	3.061(7)
mean	2.889

Ba(1)—O(1)*	4.048(11)
grand mean	3.005

lengths and bond angles in Tables 3 and 4. A list of observed and calculated structure factors can be obtained from the authors.

Description of the structures

Both structures found are in good agreement with those published by Douglass (1958) and Katscher et al. (1973) respectively, but are more accurate. In both phases [SiO_4] tetrahedra share corners to form chains with two tetrahedra in the repeat unit of the chains (*zweier* single chains) running parallel [010]. Adjacent chains are linked via every second tetrahedron to form layers (*zweier* single layers) parallel (001) (Figs. 1 and 2). In sanbornite, the low-temperature polymorph, the layers are very strongly folded. This should be expected for an anhydrous single layer silicate with a cation: silicon

Table 4. Interatomic distances (in Å) and bond angles (in °) in $Ba_2[Si_4O_{10}]$ (h). (Standard deviations in parentheses.) O*: bridging oxygen atoms

[SiO₄] tetrahedra

Si—O distances		O—O distances		O—Si—O angles	
Si(1)—O(2)	1.568(6)	O(1)*—O(4)*	2.556(8)		103.4(0.3)
—O(4)*	1.626(6)	O(1)*—O(3)*	2.596(6)		104.6(0.3)
—O(1)*	1.631(4)	O(3)*—O(4)*	2.603(8)		105.6(0.3)
—O(3)*	1.650(6)	O(2) —O(3)*	2.620(8)		109.0(0.3)
mean	1.619	O(1)*—O(2)	2.705(6)		115.4(0.3)
		O(2) ‑‑O(4)*	2.733(8)		117.6(0.3)
		mean	2.636	mean	109.3
Si(2)—O(5)	1.568(5)	O(3)*—O(4)*	2.602(8)		105.9(0.3)
—O(4)*	1.628(6)	O(4)*—O(5)	2.613(8)		109.7(0.3)
—O(3)*	1.633(6)	O(5) —O(6)*	2.617(8)		109.3(0.3)
—O(6)*	1.639(6)	O(3)*—O(6)*	2.618(9)		106.3(0.3)
mean	1.617	O(4)*—O(6)*	2.619(9)		106.6(0.3)
		O(3)*—O(5)	2.749(7)		118.4(0.3)
		mean	2.636	mean	109.4
Si(3)—O(7)	1.566(6)	O(8)*—O(8)*	2.570(5)		103.8(0.4)
—O(8)*	1.632(6)	O(6)*—O(8)*	2.600(8)		105.5(0.3)
—O(8)*	1.634(6)	O(6)*—O(7)	2.607(9)		109.0(0.3)
—O(6)*	1.635(6)	O(6)*—O(8)*	2.628(8)		107.0(0.3)
mean	1.617	O(7) —O(8)*	2.628(8)		110.5(0.3)
		O(7) —O(8)*	2.770(8)		119.9(0.3)
		mean	2.634	mean	109.3

Si—O—Si angles

Si(1)—O(3)*—Si(2)	129.0(0.3)	(2 ×)
Si(3)—O(8)*—Si(3)	135.4(0.4)	
Si(1)—O(1)*—Si(1)	136.3(0.5)	(2 ×)
Si(1)—O(4)*—Si(2)	143.1(0.4)	(2 ×)
Si(2)—O(6)*—Si(3)	143.4(0.4)	(2 ×)
mean	137.7	

[BaO]ₙ polyhedra

Ba(1)—O(5)	2.752(5)	Ba(2)—O(7)	2.702(6)
—O(5)	2.752(5)	—O(2)	2.792(6)
—O(2)	2.758(5)	—O(3)*	2.814(5)
—O(2)	2.758(5)	—O(5)	2.843(5)
—O(4)*	2.823(6)	—O(6)*	2.901(7)
—O(4)*	2.823(6)	—O(8)*	2.929(6)
—O(5)	2.991(5)	—O(7)	2.975(6)
—O(5)	2.991(5)	—O(7)	3.078(5)
mean	2.831	—O(2)	3.136(6)
		mean	2.908
Ba(1)—O(1)*	3.559(2)		
—O(1)*	3.559(2)	Ba(2)—O(6)*	4.144(7)
grand mean	2.977	grand mean	3.031

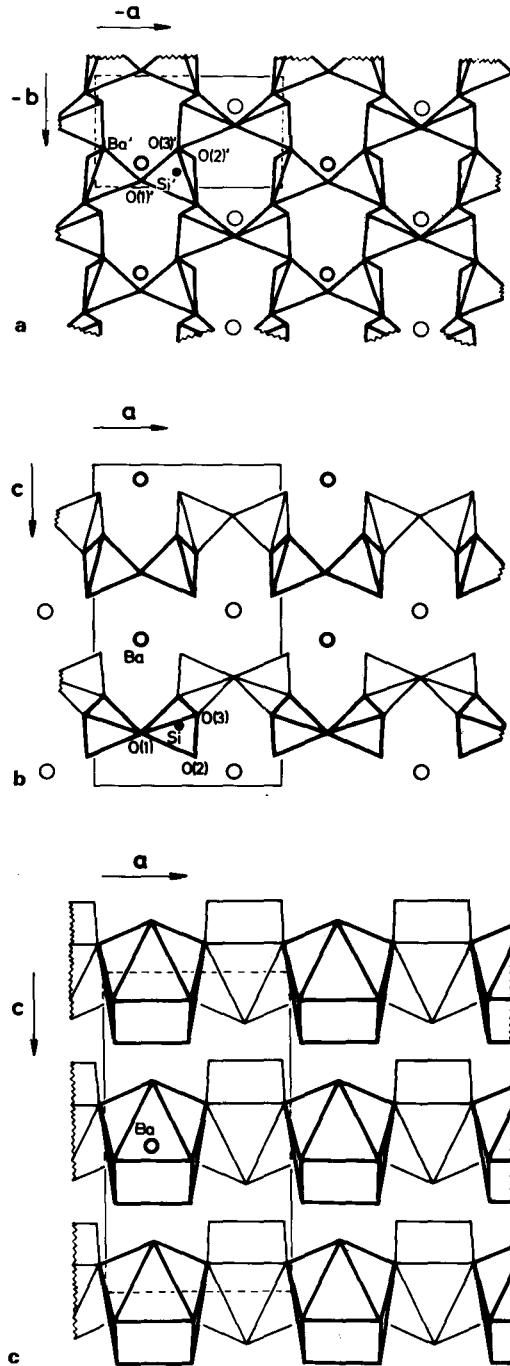**Fig. 1.**
Sanbornite, $Ba_2[Si_4O_{10}]$ (l);
a) one tetrahedral layer projected parallel [001];
b) the tetrahedral layers projected parallel [0$\bar{1}$0];
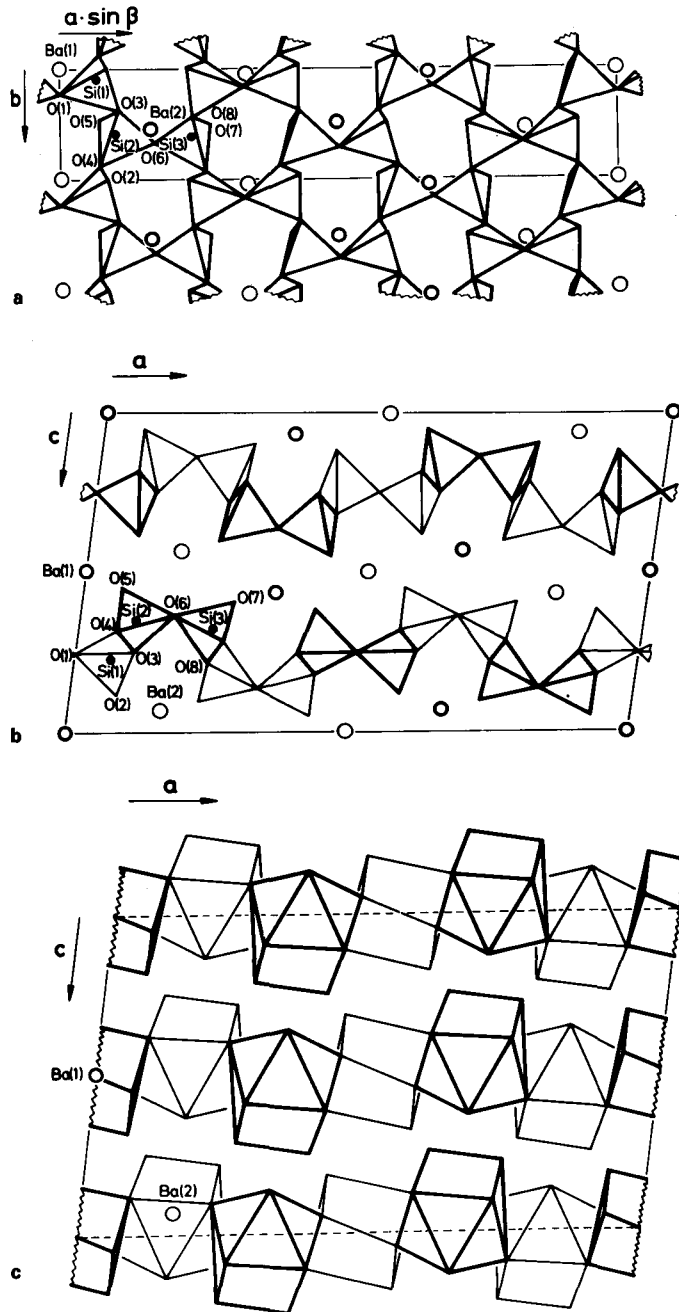c) the barium oxygen polyhedral layers projected parallel [0$\bar{1}$0]

Fig. 2. Ba$_2$[Si$_4$O$_{10}$] (h); a) one tetrahedral layer projected parallel [001]; b) the tetrahedral layers projected parallel [010]; c) the barium oxygen polyhedral layers projected parallel [010]

ratio as low as $1:2$ if the cations have to surround themselves with satisfactory coordination polyhedra of oxygen atoms that include all the terminal oxygens (Liebau, 1968). In accord with this concept, the tetrahedral layers in $Ba_2[Si_4O_{10}]$ (h) are less corrugated than those in $Ba_2[Si_4O_{10}]$ (l) as can be deduced from the values $8.90\,\text{Å}^2$ and $9.00\,\text{Å}^2$ for the areas F_T

$$= \frac{a \cdot b \cdot n_s}{n_T} \quad (n_s = \text{number of layers in the unit cell}, \ n_T = \text{number of [SiO}_4]$$

tetrahedra in the unit cell) required per $[SiO_4]$ tetrahedron of the layers in $Ba_2[Si_4O_{10}]$ (l) and (h) respectively. Both values lie well within the range assigned to anhydrous phyllosilicates by Liebau (1968). This value may be explained by the increasing effective size of the cations with increasing temperature due to higher amplitudes of their thermal vibrations.

In $Ba_2[Si_4O_{10}]$ (h) each Ba(1) ion is surrounded by six terminal oxygen atoms, O_{term}, and two bridging oxygen atoms, O^*, of the *zweier* chains, that give a centrosymmetric, slightly distorted square antiprism with Ba—O distances between 2.75 Å and 2.99 Å. This coordination is supplemented by two O^* that link adjacent *zweier* chains, their Ba—O distances being 3.56 Å. The non-symmetric coordination polyhedron around Ba(2) resembles that around Ba(1) but is considerably distorted. While six O_{term} and two O^* have distances between 2.69 Å and 3.08 Å, one of the two inter-chain bridging oxygen atoms is attracted by the barium ion to 2.90 Å, while the other is repelled to 4.14 Å.

The coordination of the Ba^{2+} ions in $Ba_2[Si_4O_{10}]$ (l) is very similar to the Ba(2) coordination in $Ba_2[Si_4O_{10}]$ (h) having six O_{term} and two intra-chain O^* between 2.73 Å and 3.06 Å, one inter-chain O^* in 3.00 Å and another one repelled to 4.05 Å.

In both polymorphs the $[BaO_n]$ polyhedra share edges to form columns parallel [010]. In the high-temperature modifcation three such columns are linked to bands and adjacent bands are joined via edges into kinked layers parallel (001) (Fig. 2c). In the low-temperature phase, in contrast, two such columns form the bands that are joined to the kinked layers parallel (001) (Fig. 1c).

References

Czank, M., Buseck, P.: Crystal chemistry of silica-rich barium silicates. II. Electron microscopy of barium silicates containing multiple chains. Z. Kristallogr. **153**, 19—32 (1980)

Douglass, R. M.: The crystal structure of sanbornite, $BaSi_2O_5$. Amer. Mineral. **43**, 517—536 (1958)

Grosse, H.-P., Tillmanns, E.: Bariummetasilicate, $BaSiO_3$ (h). Cryst. Struct. Comm. 3, 603 − 605 (1974)

Hesse, K.-F., Liebau, F.: Crystal chemistry of silica-rich barium silicates. I. Refinement of the crystal structures of $Ba_4[Si_6O_{16}]$, $Ba_5[Si_8O_{21}]$, and $Ba_6[Si_{10}O_{26}]$, silicates with triple, quadruple and quintuple chains. Z. Kristallogr. 153, 3 − 17 (1980)

Katscher, H., Bissert, G., Liebau, F.: The crystal structure of high-temperature $Ba_2[Si_4O_{10}]$. Z. Kristallogr. 137, 146 − 158 (1973)

Liebau, F.: Ein Beitrag zur Kristallchemie der Schichtsilikate. Acta Crystallogr. B24, 690 − 699 (1968)

Liebau, F.: Crystal chemistry of silica-rich barium silicates. IV. The influence of condensation degree on the crystal structure of chain and layer silicates of barium. Z. Kristallogr. in preparation (1980)